

An Efficient vLLM-Based Inference Pipeline for Unified Audio Understanding and Generation

Haoran Wang^{1,2}, Jinchuan Tian¹, Siddhant Arora¹, Shinji Watanabe^{1,**}

¹ Carnegie Mellon University
² Shanghai Jiao Tong University
haoranw5@andrew.cmu.edu

Abstract

While Large Multimodal Models excel in comprehension, high-throughput inference engines lack native support for multimodal generation. This is severe in Speech Language Models, where generating multi-layered audio tokens via decoupled AR+NAR or synchronous Multi-Token Prediction (MTP) with delay-pattern interleaving conflicts with standard single-stream loops. We present a vLLM-based inference pipeline for unified speech understanding and generation. We extend autoregressive decoding to natively execute delay-pattern de-interleaving and coordinated multi-stream sampling, integrating an on-GPU acoustic decoder for end-to-end waveform synthesis. Crucially, we overcome the shared intuition that Classifier-Free Guidance (CFG) halves throughput. By co-scheduling paired conditional and unconditional requests within a continuous batch, our CFG implementation sustains 80% of non-CFG throughput, absorbing dual-request and logit merging overheads. We open-source our framework¹.

Index Terms: Speech Language Models, High-Throughput Inference, End-to-End Speech Generation

1. Introduction

The rapid evolution of Large Language Models (LLMs) has transitioned artificial intelligence from text-only interfaces to rich, multimodal interactions. Recently, Speech Language Models (SpeechLMs) [1, 2, 3, 4] have emerged as a pivotal frontier for unified audio understanding and generation. By modeling continuous audio signals as discrete acoustic tokens [5, 6, 7], these models bypass traditional cascaded Automatic Speech Recognition (ASR) [8] and Text-to-Speech (TTS) [9, 10] pipelines to achieve strong and expressive acoustic capabilities. Building upon this end-to-end foundation, advanced interactive features like direct speech-to-speech dialogue [11, 12] naturally emerge as downstream applications.

However, the deployment of SpeechLMs exposes a structural gap in current high-throughput inference engines. While state-of-the-art serving frameworks [13, 14] excel at memory efficiency and dynamic request scheduling (e.g., continuous batching [15] and automatic prefix caching [14]), their underlying mechanisms were largely optimized for unimodal, text-only generation. Consequently, extending this text-centric architecture to handle the continuous and distinct nature of speech outputs introduces significant bottlenecks.

Generating general audio diverges from standard text autoregression in two critical aspects:

- 1. Multi-Layered Token Generation and Decoding.** Unlike text, continuous speech is typically compressed by neural audio codecs [5, 7, 16, 17]. Modern SpeechLMs favor Residual Vector Quantization (RVQ), encoding each temporal frame into multi-layered tokens to support high-fidelity audio at a constant frame rate. To model this multi-codebook grid, current paradigms primarily adopt synchronous Multi-Token Prediction (MTP) [3] and delay-pattern interleaving [1, 18]. While delay-pattern elegantly flattens tokens for training, its inference demands multi-stream sampling and complex de-interleaving. Furthermore, synthesizing the final waveform requires an auxiliary acoustic decoder (vocoder). Coupling MTP with this additional decoding stage inherently conflicts with the standard one-token-per-step serving loop.
- 2. The Classifier-Free Guidance (CFG) Bottleneck.** Classifier-Free Guidance (CFG) [19] is essential for high-fidelity audio generation, as evidenced by its widespread adoption in various audio synthesis frameworks [18, 20, 21]. Mechanistically, implementing CFG requires two parallel forward passes per step: one conditioned on the input prompt and one unconditional. This dual-pass requirement inherently doubles computational and memory overheads. Since standard schedulers assume strict request independence, they lack native mechanisms to coordinate these paired passes. Consequently, naive implementations are forced to process them as separate requests. This disjoint scheduling duplicates KV cache allocations and precludes joint batching. Furthermore, the necessary logit merging must operate across disjoint request contexts with explicit synchronization. The compounding of these dual-request overheads and synchronization costs can severely degrade overall system throughput.

To bridge this gap, we present a novel inference implementation engineered for the unified understanding and generation of audio. Built upon vLLM [13] which is a high-performance continuous batching backend, our framework extends the autoregressive decoding loop to natively support synchronous multi-stream sampling with delay-pattern de-interleaving for multi-codebook audio generation. Furthermore, we fuse a lightweight acoustic decoder directly into the engine’s output pipeline, enabling single-process audio synthesis without an external vocoder service.

To address the CFG overhead, we introduce a Paired Request Co-Scheduling mechanism. By co-scheduling paired conditional and unconditional requests within the same continuous batch, our approach ensures them to share a single forward pass through the transformer backbone. This unified execution elegantly absorbs the dual-request and logits merging overheads, directly overcoming the shared intuition that CFG inevitably halves system throughput.

^{**}indicates the corresponding author.

¹<https://github.com/whr-a/vllm/tree/opuslm>

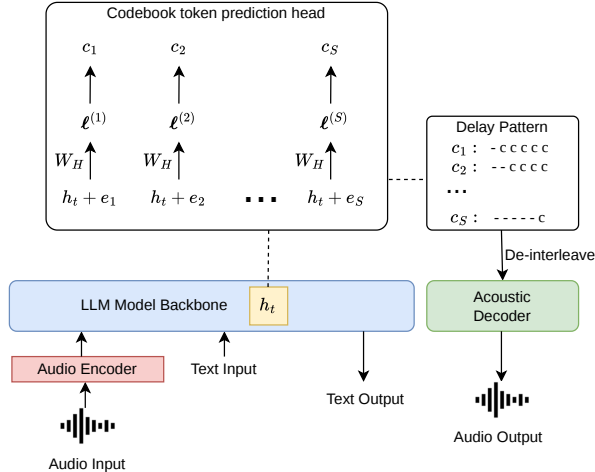


Figure 1: *Speech language model architecture. The unified autoregressive transformer processes encoded audio and text. During audio generation, hidden states h_t and stream embeddings e_i (where $1 \leq i \leq S$) are projected via S codebook heads into parallel delayed streams, which are subsequently de-interleaved for acoustic decoding.*

The main contributions are summarized as follows.

1. We identify the structural limitations of current text-centric inference engines in handling multimodal auto-regressive generation and propose a unified architecture that natively supports synchronous multi-stream sampling and delay-pattern de-interleaving for multi-codebook audio tokens.
2. We design an end-to-end fused acoustic pipeline that integrates a lightweight audio decoder directly into the engine’s output pipeline, eliminating the need for an external vocoder service and enabling single-process waveform synthesis on GPU.
3. We introduce a Paired Request Co-Scheduling strategy for CFG. By systematically pairing and co-scheduling conditional and unconditional requests within the same continuous batch, our system efficiently absorbs dual-branch overheads and logit synchronization costs, sustaining up to 80% of non-CFG throughput and effectively overcoming the shared intuition of halved performance, while seamlessly supporting the concurrent prefilling and decoding of text and CFG-enabled audio requests in a unified pipeline.

2. Method

We present a serving framework that enables high-throughput inference for unified audio understanding and generation within existing token-level continuous batching engines. We first describe the class of models our framework targets (§2.1), then detail our unified serving pipeline (§2.3), and finally describe efficient Classifier-Free Guidance (§2.4).

2.1. Speech Language Models

Our system broadly targets the widely adopted *delay-pattern* [18] SpeechLM architecture. To validate the generality of our pipeline, we ground our implementation and evaluation in three representative models: Bagpiper [1], OpusLM [2], and OpusLM dialogue [11]. As illustrated in Figure 1, the core generation mechanisms of these models share a unified architec-

tural foundation.

Multi-token Prediction. The pipeline begins with an audio encoder feeding continuous speech to an autoregressive LLM. The LLM operates over a unified vocabulary, partitioned into text and S audio sub-vocabulary. For audio output, at each time step t , the LLM backbone produces a hidden state h_t . As illustrated in Figure 1, S parallel codebook heads then project this state to generate logits $\ell^{(i)}$ and their corresponding sampled tokens c_i (where $1 \leq i \leq S$). Specifically, each head adds a learnable stream embedding e_i to h_t before applying a shared language modeling head W_H , such that $\ell^{(i)} = W_H(h_t + e_i)$.

Delay Interleave pattern. Under the delay pattern [18], the i -th stream is offset by i steps, meaning the S tokens $\{c_1, \dots, c_S\}$ emitted at step t correspond to different temporal positions. To maintain this structure during autoregressive feedback, the input representation at each step aggregates the embeddings of these previously generated tokens. Post-generation, the resulting $S \times T$ codebook matrix (where T represents the total number of acoustic frames) is de-interleaved and passed to an acoustic decoder for waveform synthesis. Crucially, this unified vocabulary inherently enables mixed-modality responses (e.g., text seamlessly transitioning to audio).

2.2. Standard Continuous Batching Engines

Modern text-based LLM serving frameworks, such as vLLM [13], maximize hardware utilization through iteration-level scheduling and continuous batching. Rather than processing static batches where early-finishing requests idle, the scheduler dynamically injects new prompts and retires completed generations at the granularity of a single decoding step. This highly dynamic scheduling is supported by memory management mechanisms like PagedAttention [13], which partitions the Key-Value (KV) cache into fixed-size, non-contiguous blocks to allocate GPU memory on demand and eliminate fragmentation. Structurally, these engines treat the underlying model as a black box that executes a uniform forward pass across all active requests. Consequently, the entire system infrastructure is deeply coupled to the assumption of homogeneous, single-stream text generation, presenting a strict architectural constraint that our framework must navigate to support multi-token prediction and CFG inference.

2.3. Unified Multi-Token Prediction Serving Pipeline

To navigate this single-stream constraint and support S parallel audio tokens without requiring pervasive modifications to the engine’s iteration-level scheduler or PagedAttention [13] infrastructure, we introduce a *primary-auxiliary decomposition*, as depicted in Figure 2 (Left).

Primary-Auxiliary Decomposition. We designate one codebook stream as the *primary* token, which is fully managed by the engine’s standard pipeline. The remaining $S-1$ *auxiliary* streams are sampled internally during the model’s logit computation and buffered per-request. Consequently, the model appears to the engine as a standard text LM that emits a single token per step, while transparently executing the multi-codebook generation.

De-interleave and Decode. Upon request completion, the buffered matrix is delay-de-interleaved and passed to a co-located on-GPU acoustic decoder, fusing waveform synthesis directly into the serving path.

Mixed-Modality Phase Management. To orchestrate mixed text-audio outputs within this token-level engine, we implement a per-request *phase state machine* enforced via dy-

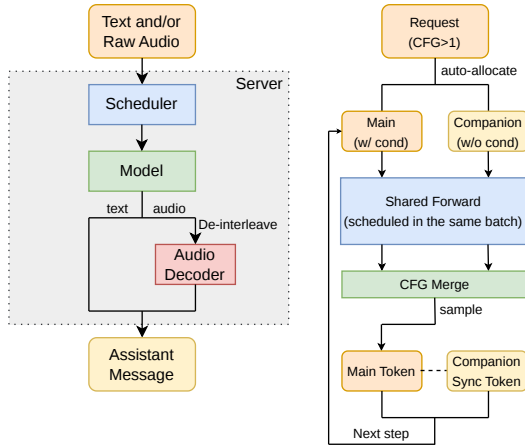


Figure 2: *Unified serving framework for SpeechLMs. (Left) Overall pipeline: The engine manages continuous batching, primary-auxiliary token generation, and fused on-GPU acoustic decoding for mixed-modality streaming. (Right) Paired co-scheduling for CFG: Conditional and unconditional requests share a batched forward pass, merging logits before sampling and synchronizing the sampled token for the next step.*

dynamic vocabulary masking. The system transitions across three main states: a *text phase* restricted to text tokens, a *transition phase* injecting deterministic bridging tokens to condition audio generation, and an *audio phase* activating all S streams. Crucially, terminating the audio phase initiates a *drain sub-phase* that emits $S-1$ padding tokens to flush the delay buffer, guaranteeing a complete $S \times T$ codebook matrix (where T represents the total number of acoustic frames) for de-interleaving. Furthermore, because continuous batching interleaves tokens from multiple requests into a single flattened sequence, tracking modality via input positions is unreliable. We bypass this by dynamically inferring the active modality directly from the model’s unmasked output distribution (i.e., the argmax over the disjoint vocabulary regions), ensuring robust and engine-agnostic phase management.

2.4. Classifier-Free Guidance via Paired Request Co-Scheduling

Classifier-Free Guidance (CFG) [19] improves audio fidelity by interpolating between conditional and unconditional distributions. Building upon the logit formulation $\ell^{(i)}$ defined in Section 2.3, we apply CFG independently to each codebook stream i :

$$\tilde{\ell}^{(i)} = w \cdot \ell_{\text{cond}}^{(i)} + (1 - w) \cdot \ell_{\text{uncond}}^{(i)}, \quad w > 1 \quad (1)$$

A straightforward implementation would issue two independent requests, incurring severe scheduling fragmentation and cross-request synchronization overhead, and is not feasible because it needs step-by-step sync. To resolve this, we introduce *paired request co-scheduling*, which natively coordinates this dual-pass requirement within the serving engine.

As detailed in Figure 2 (Right), the end-to-end processing pipeline begins with the input auto-allocation: when the server receives a request with a CFG scale $w > 1$, it transparently generates a “Companion” request (with a null prompt) alongside the “Main” conditional request. The engine treats this pair as an atomic scheduling unit and always process them together. During the shared forward process, they are co-scheduled into the

same continuous batch and share a single forward pass through the transformer backbone. The engine strictly partitions the per-step token budget equally between the pair.

After the forward pass, the raw logits $\ell_{\text{cond}}^{(i)}$ and $\ell_{\text{uncond}}^{(i)}$ from both contexts are merged according to Eq. 1. Crucially, this CFG merge operates only during the audio phase; it bypasses modality-switching tokens to prevent CFG from corrupting the phase state machine. To avoid redundant compute, projections for auxiliary streams are batched together.

Finally, for the output and synchronization step, the engine samples a single Main Token from the merged distribution $\tilde{\ell}^{(i)}$. To ensure both contexts maintain the exact same autoregressive history for the next step, this sampled token is synchronously appended to the Companion request, while the companion’s external outputs remain hidden from the client. By systematically co-scheduling these pairs within the same continuous batch, our architecture efficiently absorbs the dual-branch overheads and logit synchronization costs. This design effectively overcomes the conventional assumption that CFG halves performance, allowing the system to sustain up to 80% of non-CFG throughput.

3. Experiment

3.1. Experimental Setup

We evaluate our framework on three fully open-source SpeechLM architectures that span different design points, all sharing a delay-pattern codec structure and supporting both audio understanding and generation:

- **Bagpiper** [1]: A model utilizing a Qwen3-8B [22] backbone with 8 parallel codebook streams encoded via X-Codec [6]. It is designed for open-ended audio understanding and generation, natively supporting Classifier-Free Guidance for high-fidelity audio synthesis.
- **OpusLM** [2]: A model featuring an OLMo-2-7B [23] backbone with a 9-stream setup (1 SSL [24] + 8 DAC [5, 25]), tailored for both ASR and TTS tasks.
- **OpusLM-Dialogue** [11]: A model adopting a SmolLM2-1.7B [26] backbone. It retains the same 9-stream codec configuration as OpusLM but is specifically optimized for spoken dialogue tasks.

For the baseline, we use the original PyTorch inference pipeline, which processes requests sequentially without continuous batching. All experiments are conducted on a single NVIDIA H100 80GB GPU with FlashAttention-3 [27] enabled. The maximum model sequence length is set to 16,384 tokens for all configurations. To maximize operational efficiency and fully saturate the GPU, we maintain a concurrency level of 512 simultaneous requests for standard evaluations. For CFG-enabled settings, the concurrency is proportionally adjusted to 256 requests to account for the internal companion requests, yielding an equivalent active workload. This targeted concurrency ensures that the serving engine maintains a steady, moderately sized queue to sustain peak overall throughput.

3.2. Throughput

In addition to decode token rates, we measure Model FLOPs Utilization (MFU), which quantifies the ratio of actual floating-point operations to the GPU’s theoretical peak capacity, providing a standardized metric for hardware utility. As summarized in Table 1, our continuous-batching pipeline achieves massive performance gains over the sequential PyTorch baseline across all models. By effectively batching multi-stream generation, our system accelerates token processing speeds by

Table 1: *Prompt and generation throughput comparison. All measurements are conducted on a single H100 80GB GPU with FlashAttention-3 and a maximum sequence length of 16,384.*

System	Decode (tok/s)	MFU (%)
Bagpiper (PyTorch)	52.7	0.096
Bagpiper (vLLM)	5694.5	9.95
OpusLM (PyTorch)	36.5	0.311
OpusLM (vLLM)	4582.9	9.89
OpusLM-Dial. (PyTorch)	53.9	0.290
OpusLM-Dial. (vLLM)	5870.5	3.28

roughly two orders of magnitude. This architectural advantage directly translates to hardware utilization: while the baseline severely underutilizes the H100 GPU with an MFU well below 0.1%, our serving engine efficiently absorbs scheduling overheads to drive the MFU up to 9.95% for Bagpiper and 9.89% for OpusLM. Notably, the 1.7B parameter OpusLM dialogue model exhibits a lower MFU of 3.28% despite achieving the highest absolute token throughput. This occurs because such a compact model possesses low arithmetic intensity on the H100 GPU, causing inference to hit the memory bandwidth wall before fully saturating the compute units.

3.3. Numerical and Quality Check

A prerequisite for any serving optimization is that it must not degrade model output quality. We verify numerical correctness using the Bagpiper model [1] on the MMAU-mini dataset [28]. Specifically, we compare the token sequences and logit distributions produced by our continuous-batching pipeline against the reference PyTorch implementation under identical inputs and random seeds.

Table 2: *Numerical deviation against the reference PyTorch implementation.*

Configuration	RMSE (Max)	RMSE (Mean)	First Mismatch
FP32 + SDPA [29]	0.081	0.008	None (Identical)
BF16 + FA3 [27]	0.532	0.163	34.0

As shown in Table 2, under Float32 precision, the two implementations produce strictly identical token sequences, with a negligible mean logit RMSE of 0.008. This exact alignment confirms that our custom multi-stream sampling and phase control introduce no numerical bugs. When transitioning to BF16 with FlashAttention-3 [27], a mismatch occurs around step 34, increasing the mean RMSE to 0.163. This discrepancy is an expected consequence of precision loss and non-associative floating-point arithmetic [30, 31].

Crucially, this inherent hardware-level divergence does not negatively impact end-to-end model fidelity. To confirm this empirically, we evaluate inference quality across understanding and generation tasks, as summarized in Table 3. We report accuracy on MMAU-mini [28] and word error rate (WER) on LibriSpeech test-clean [32] for understanding. For generation, we report WER on LibriSpeech test-clean and UTMOS on the Eval2000 dataset. While minor instance-level variations in synthesized speech naturally arise from hardware precision shifts and the inherent variance of TTS generation, outputs produced by our pipeline safely maintain the expected aggregate performance of the underlying models across all metrics.

Table 3: *Inference quality evaluation. Understanding is measured by MMAU-mini accuracy (%), \uparrow and ASR word error rate (%), \downarrow . Generation is measured by TTS word error rate (%), \downarrow and dialogue UTMOS (\uparrow). “–” indicates the task is not supported by the model.*

System	Understanding		Generation	
	MMAU-mini \uparrow	ASR \downarrow	TTS \downarrow	UTMOS \uparrow
Bagpiper (PyTorch)	74.5	2.5	2.7	–
Bagpiper (vLLM)	75.4	2.6	3.3	–
OpusLM (PyTorch)	–	2.3	4.6	–
OpusLM (vLLM)	–	1.9	5.3	–
OpusLM-Dial. (PyTorch)	–	–	–	2.85
OpusLM-Dial. (vLLM)	–	–	–	2.51

Table 4: *CFG overhead on Bagpiper (vLLM). Prompt and generation throughput (tok/s) and MFU (%) with and without Classifier-Free Guidance.*

Setting	Prefill (tok/s)	Decode (tok/s)	MFU (%)
w/o CFG	315.8	4952.0	8.0
w/ CFG	271.2	3960.7	12.8

3.4. CFG Overhead Analysis

While CFG inherently doubles compute via parallel forward passes, Table 4 shows our co-scheduling sustains over 80% of baseline throughput. These measurements are conducted using Bagpiper on the LibriSpeech TTS task, operating at concurrencies of 256 and 512 for the CFG and baseline configurations, respectively. This efficiency stems from three factors. First, the companion request strictly copies the main sequence, ensuring near-perfect prefix cache hits and minimizing KV cache overhead. Second, since autoregressive decoding is fundamentally memory-bound, processing the companion request merely constitutes a marginal addition to the active batch size. This saturates idle compute to boost MFU with negligible latency and synchronization penalties. Finally, models like Bagpiper generate extensive textual reasoning before brief audio outputs. Selectively activating CFG solely during this short audio phase effectively amortizes the dual-pass cost across the entire end-to-end sequence.

4. Conclusion

In this work, we presented a unified inference architecture that extends a continuous batching engine to natively support Speech Language Models. By integrating synchronous multi-stream sampling and delay-pattern de-interleaving into the generation loop, our design effectively handles the complexities of multi-layered audio tokens. Through a *Paired Request Co-Scheduling* strategy, our system efficiently absorbs dual-branch overheads, sustaining 80% of non-CFG throughput. Experimental results across multiple SpeechLM architectures demonstrate up to $108\times$ generation throughput improvement over sequential PyTorch inference while maintaining strict numerical correctness. As the modifications remain confined to the model and logit processing layers, this architecture provides a portable and high-performance foundation for real-time multimodal voice applications.

5. Generative AI Use Disclosure

Artificial intelligence tools were utilized exclusively for language editing and manuscript polishing. The core technical contributions, including the system architecture design, framework implementation, and experimental evaluation, were independently conducted by the authors.

6. Acknowledgment

This work used the Bridges2 at PSC and Delta/DeltaAI NCSA systems through CIS210014 from the ACCESS program, supported by NSF #2138259, #2138286, #2138307, #2137603, and #2138296.

7. References

- [1] J. Tian, H. Wang, B.-H. Su, C.-y. Huang, Q. Wang, J. Shi, W. Chen, X. Gong, S. Arora, C.-J. Li *et al.*, “Bagpiper: Solving open-ended audio tasks via rich captions,” *arXiv preprint arXiv:2602.05220*, 2026.
- [2] J. Tian, W. Chen, Y. Peng, J. Shi, S. Arora, S. Bharadwaj, T. Maekaku, Y. Shinohara, K. Goto, X. Yue *et al.*, “Opuslm: A family of open unified speech language models,” *arXiv preprint arXiv:2506.17611*, 2025.
- [3] J. Xu, Z. Guo, H. Hu, Y. Chu, X. Wang, J. He, Y. Wang, X. Shi, T. He, X. Zhu *et al.*, “Qwen3-omni technical report,” *arXiv preprint arXiv:2509.17765*, 2025.
- [4] D. Ding, Z. Ju, Y. Leng, S. Liu, T. Liu, Z. Shang, K. Shen, W. Song, X. Tan, H. Tang *et al.*, “Kimi-audio technical report,” *arXiv preprint arXiv:2504.18425*, 2025.
- [5] J. Shi, J. Tian, Y. Wu, J.-w. Jung, J. Q. Yip, Y. Masuyama, W. Chen, Y. Wu, Y. Tang, M. Baali *et al.*, “Espnet-codec: Comprehensive training and evaluation of neural codecs for audio, music, and speech,” in *2024 IEEE Spoken language technology workshop (SLT)*. IEEE, 2024, pp. 562–569.
- [6] Z. Ye, P. Sun, J. Lei, H. Lin, X. Tan, Z. Dai, Q. Kong, J. Chen, J. Pan, Q. Liu *et al.*, “Codec does matter: Exploring the semantic shortcoming of codec for audio language model,” in *Proceedings of the AAAI Conference on Artificial Intelligence*, vol. 39, no. 24, 2025, pp. 25 697–25 705.
- [7] H. Wang, J. Shi, J. Tian, B. Li, K. Yu, and S. Watanabe, “Bscodec: A band-split neural codec for high-quality universal audio reconstruction,” *arXiv preprint arXiv:2511.06150*, 2025.
- [8] A. Radford, J. W. Kim, T. Xu, G. Brockman, C. McLeavey, and I. Sutskever, “Robust speech recognition via large-scale weak supervision,” in *International conference on machine learning*. PMLR, 2023, pp. 28 492–28 518.
- [9] J. Kim, J. Kong, and J. Son, “Conditional variational autoencoder with adversarial learning for end-to-end text-to-speech,” in *International conference on machine learning*. PMLR, 2021, pp. 5530–5540.
- [10] J. Shen, R. Pang, R. J. Weiss, M. Schuster, N. Jaitly, Z. Yang, Z. Chen, Y. Zhang, Y. Wang, R. Skerrv-Ryan *et al.*, “Natural tts synthesis by conditioning wavenet on mel spectrogram predictions,” in *2018 IEEE international conference on acoustics, speech and signal processing (ICASSP)*. IEEE, 2018, pp. 4779–4783.
- [11] S. Arora, J. Tian, J. Shi, H. Futami, Y. Kashiwagi, E. Tsunoo, and S. Watanabe, “Optimizing conversational quality in spoken dialogue systems with reinforcement learning from ai feedback,” *arXiv preprint arXiv:2601.19063*, 2026.
- [12] A. Défossez, L. Mazaré, M. Orsini, A. Royer, P. Pérez, H. Jégou, E. Grave, and N. Zeghidour, “Moshi: a speech-text foundation model for real-time dialogue,” *arXiv preprint arXiv:2410.00037*, 2024.
- [13] W. Kwon, Z. Li, S. Zhuang, Y. Sheng, L. Zheng, C. H. Yu, J. E. Gonzalez, H. Zhang, and I. Stoica, “Efficient memory management for large language model serving with pagedattention,” in *Proceedings of the ACM SIGOPS 29th Symposium on Operating Systems Principles*, 2023.
- [14] L. Zheng, L. Yin, Z. Xie, C. L. Sun, J. Huang, C. H. Yu, S. Cao, C. Kozyrakis, I. Stoica, J. E. Gonzalez *et al.*, “Sglang: Efficient execution of structured language model programs,” *Advances in neural information processing systems*, vol. 37, pp. 62 557–62 583, 2024.
- [15] G.-I. Yu, J. S. Jeong, G.-W. Kim, S. Kim, and B.-G. Chun, “Orca: A distributed serving system for {Transformer-Based} generative models,” in *16th USENIX symposium on operating systems design and implementation (OSDI 22)*, 2022, pp. 521–538.
- [16] P. Mousavi, G. Maimon, A. Moumen, D. Petermann, J. Shi, H. Wu, H. Yang, A. Kuznetsova, A. Ploujnikov, R. Marxer *et al.*, “Discrete audio tokens: More than a survey!” *arXiv preprint arXiv:2506.10274*, 2025.
- [17] Y. Guo, Z. Li, H. Wang, B. Li, C. Shao, H. Zhang, C. Du, X. Chen, S. Liu, and K. Yu, “Recent advances in discrete speech tokens: A review,” *IEEE Transactions on Pattern Analysis and Machine Intelligence*, 2025.
- [18] J. Copet, F. Kreuk, I. Gat, T. Remez, D. Kant, G. Synnaeve, Y. Adi, and A. Défossez, “Simple and controllable music generation,” *Advances in neural information processing systems*, vol. 36, pp. 47 704–47 720, 2023.
- [19] J. Ho and T. Salimans, “Classifier-free diffusion guidance,” *arXiv preprint arXiv:2207.12598*, 2022.
- [20] J. Tian, S.-g. Lee, Z. Kong, S. Ghosh, A. Goel, C.-H. H. Yang, W. Dai, Z. Liu, H. Ye, S. Watanabe *et al.*, “Ualm: Unified audio language model for understanding, generation and reasoning,” *arXiv preprint arXiv:2510.12000*, 2025.
- [21] H. Liu, Z. Chen, Y. Yuan, X. Mei, X. Liu, D. Mandic, W. Wang, and M. D. Plumbley, “Audioldm: Text-to-audio generation with latent diffusion models,” *arXiv preprint arXiv:2301.12503*, 2023.
- [22] A. Yang, A. Li, B. Yang, B. Zhang, B. Hui, B. Zheng, B. Yu, C. Gao, C. Huang, C. Lv *et al.*, “Qwen3 technical report,” *arXiv preprint arXiv:2505.09388*, 2025.
- [23] T. OLMo, P. Walsh, L. Soldaini, D. Groeneveld, K. Lo, S. Arora, A. Bhagia, Y. Gu, S. Huang, M. Jordan *et al.*, “2 olmo 2 furious,” *arXiv preprint arXiv:2501.00656*, 2024.
- [24] W. Chen, W. Zhang, Y. Peng, X. Li, J. Tian, J. Shi, X. Chang, S. Maiti, K. Livescu, and S. Watanabe, “Towards robust speech representation learning for thousands of languages,” in *Proceedings of the 2024 Conference on Empirical Methods in Natural Language Processing*, 2024, pp. 10 205–10 224.
- [25] R. Kumar, P. Seetharaman, A. Luebs, I. Kumar, and K. Kumar, “High-fidelity audio compression with improved rvqgan,” *Advances in Neural Information Processing Systems*, vol. 36, pp. 27 980–27 993, 2023.
- [26] L. B. Allal, A. Lozhkov, E. Bakouch, G. M. Blázquez, G. Penedo, L. Tunstall, A. Marafioti, H. Kydlíček, A. P. Lajarín, V. Srivastav *et al.*, “Smolm2: When smol goes big—data-centric training of a small language model,” *arXiv preprint arXiv:2502.02737*, 2025.
- [27] J. Shah, G. Bikshandi, Y. Zhang, V. Thakkar, P. Ramani, and T. Dao, “Flashattention-3: Fast and accurate attention with asynchrony and low-precision,” *Advances in Neural Information Processing Systems*, vol. 37, pp. 68 658–68 685, 2024.
- [28] S. Sakshi, U. Tyagi, S. Kumar, A. Seth, R. Selvakumar, O. Nieto, R. Duraiswami, S. Ghosh, and D. Manocha, “Mmau: A massive multi-task audio understanding and reasoning benchmark,” *arXiv preprint arXiv:2410.19168*, 2024.
- [29] A. Vaswani, N. Shazeer, N. Parmar, J. Uszkoreit, L. Jones, A. N. Gomez, Ł. Kaiser, and I. Polosukhin, “Attention is all you need,” *Advances in neural information processing systems*, vol. 30, 2017.
- [30] A. Golden, S. Hsia, F. Sun, B. Acun, B. Hosmer, Y. Lee, Z. De-Vito, J. Johnson, G.-Y. Wei, D. Brooks *et al.*, “Is flash attention stable?” *arXiv preprint arXiv:2405.02803*, 2024.

- [31] J. Yuan, H. Li, X. Ding, W. Xie, Y.-J. Li, W. Zhao, K. Wan, J. Shi, X. Hu, and Z. Liu, "Understanding and mitigating numerical sources of nondeterminism in llm inference," *arXiv preprint arXiv:2506.09501*, 2025.
- [32] V. Panayotov, G. Chen, D. Povey, and S. Khudanpur, "Librispeech: an asr corpus based on public domain audio books," in *2015 IEEE international conference on acoustics, speech and signal processing (ICASSP)*. IEEE, 2015, pp. 5206–5210.